Ecotoxicology and Environmental Safety 211 (2021) 111930

Contents lists available at ScienceDirect

Ecotoxicology and Environmental Safety

journal homepage: www.elsevier.com/locate/ecoenv

Evaluation of the effect of silver and silver nanoparticles on the function of selenoproteins using an in-vitro model of the fish intestine: The cell line RTgutGC

Debarati Chanda [a], William Dudefoi [a,b], Joshua Anadu [a], Matteo Minghetti [a,*]

[a] Department of Integrative Biology, Oklahoma State University, Stillwater, OK, USA
[b] Department of Earth and Planetary Sciences, Washington University, Saint Louis, MO, USA

ARTICLE INFO

Edited by Professor Bing Yan

Keywords:
AgNO3
AgNP
Glutathione peroxidase
Thioredoxin reductase
RTgutGC
Oxidative stress
Selenoproteins

ABSTRACT

Emerging research in mammalian cells suggests that ionic ($AgNO_3$) and nano silver (AgNP) can disrupt the metabolism of selenium which plays a vital role in oxidative stress control. However, the effect of silver (Ag) on selenoprotein function in fish is poorly understood. Here we evaluate the effects of $AgNO_3$ and citrate coated AgNP (cit-AgNP) on selenoprotein function and oxidative stress using a fish cell line derived from the rainbow trout (*Oncorhynchus mykiss*) intestine (RTgutGC). Cell viability was evaluated using a cytotoxicity assay which measures simultaneously metabolic activity, membrane integrity and lysosome integrity. Cells exposed to equimolar amounts of $AgNO_3$ and cit-AgNP accumulated the same amount of silver intracellularly, however $AgNO_3$ was more toxic than cit-AgNP. Selenoenzymes glutathione peroxidase (GPx) and thioredoxin reductase (TrxR) mRNA levels and enzyme activity were measured. While mRNA levels remained unaffected by $AgNO_3$ or cit-AgNP, the enzyme activity of GPx was inhibited by $AgNO_3$ (1 μM) and cit-AgNP (5 μM) and TrxR activity was inhibited by $AgNO_3$ (0.4 μM) and cit-AgNP (1, 5 μM). Moreover, cells exposed to 1 μM of $AgNO_3$ and cit-AgNP showed an increase in metallothionein b (MTb) mRNA levels at 24 h of exposure, confirming the uptake of silver, but returned to control levels at 72 h suggesting silver scavenging by MTb. Oxidative stress was not observed at any of the doses of $AgNO_3$ or cit-AgNP tested. Overall, this study shows that $AgNO_3$ or cit-AgNP can inhibit the activity of selenoenzymes but do not induce oxidative stress in RTgutGC cells.

1. Introduction

Due to its antimicrobial properties silver is used in several medical applications (Lemire et al., 2013). Moreover, the emergence of antibiotic resistance in aquatic microbes has contributed to a renewed interest in developing alternative methods of control and prevention of diseases in aquaculture. Among the alternative methods, AgNP have been considered due to their potential in controlling pathogens and relatively low acute fish toxicity and have been applied in aquaculture as a disease control agent (Fuentes-Valencia et al., 2020; Swain et al., 2014). This represents a potential for direct exposure of farmed fish. In addition, the waste generated from Ag products can eventually permeate waterbodies (Tortella et al., 2020), which might result in a source of exposure for aquatic organisms. Presence of Ag in different waterbodies is a concern and measurement of Ag in organs of aquatic organisms including cetaceans, fish and gastropods have been reported (Cáceres-Saez et al., 2019; Jiang et al., 2017; Petersen, 2017). This raises questions on whether the exponential demand for AgNPs in commercial and medical products can actually have a deleterious effect on aquatic species health (Piccinno et al., 2012). It has been previously reported that exposure to water contaminated with AgNP results in accumulation of Ag in fish tissues specifically gill, gut and liver which are primary target organs (Clark et al., 2019a; Xiao et al., 2020). In zebrafish, AgNPs were mainly taken up via oral ingestion suggesting that the intestine is an important target organ for AgNP exposures (Xiao et al., 2020). Previously, Ag nanotoxicology studies have been conducted on the gill epithelium in-vivo (Bruneau et al., 2016; Schultz et al., 2012) and in-vitro (Farkas et al., 2011; Yue et al., 2015), while the intestinal epithelium has not been investigated as much due to the lack of an appropriate model (Clark et al., 2019b; Minghetti and Schirmer, 2016). This is particularly relevant given that the intestine is a major route of absorption of pollutants in fish living in brackish or sea water (Evans, 2008).

* Correspondence to: Department of Integrative Biology, Oklahoma State University, 501 Life Sciences West, Stillwater, OK 74078, USA.
E-mail address: matteo.minghetti@okstate.edu (M. Minghetti).

https://doi.org/10.1016/j.ecoenv.2021.111930
Received 23 September 2020; Received in revised form 21 December 2020; Accepted 10 January 2021
Available online 17 January 2021

Silver is a known toxicant in fish due to its inhibitory effect on the Na^+/K^+-ATPase and intracellular carbonic anhydrase in the ionocytes (Wood, 2011). Na^+/K^+-ATPase inhibition was also shown for AgNP (Schultz et al., 2012). This effect depletes the Na^+ and Cl^- concentration in the blood plasma resulting in circulatory collapse and mortality (Wood, 2011). Moreover, Ag is a toxicant for several antioxidant enzymes such as catalase (CAT), glutathione peroxidase (GPx), superoxide dismutase (SOD) and thioredoxin reductase (TrxR), which play an important role in protecting the cells against oxidative stress (Barros et al., 2019). Notably, GPx and TrxR belong to the protein family of selenoproteins that incorporate selenium in the form of selenocysteine as a catalytic co-factor (Burk and Hill, 2005; Labunskyy et al., 2014). It has been shown that TrxR enzyme activity is inhibited by Ag and AgNP exposure and that Ag ions and AgNP decreased selenium (Se) incorporation during TrxR synthesis in mammalian keratinocyte (HaCat) and lung (A549) cells in a dose-dependent manner (Srivastava et al., 2012). This finding indicates that antioxidant enzymes could be inhibited on interaction with Ag - a potential mechanism by which Ag causes detrimental intracellular effects. Given that this effect was observed on TrxR, Ag could be inducing similar effects on other antioxidant enzymes such as GPx (Habas and Shang, 2019; Srivastava et al., 2012). While much of the research on the effect of Ag on selenoenzymes has mainly focused on mammalian systems (Gmoshinski et al., 2016; Khan et al., 2019; Srivastava et al., 2012), the role of Ag on selenoenzymes in environmental species, such as fish, is less understood. Previously, it was shown that the expression of two genes involved in oxidative stress and selenium metabolism, such as Selenoprotein P and thioredoxin-interacting protein (TXNIP), were affected by AgNP exposure in vivo in Nile Tilapia (*Oreochromis niloticus*) (Thummabancha et al., 2016). A downregulation in the selenoprotein P expression and an upregulation in TXNIP suggested that AgNP suppressed the expression of the key antioxidant proteins in target organs like liver, intestine, peripheral blood leukocytes, brain and gills (Thummabancha et al., 2016). This study indicates that $AgNO_3$ and AgNP induce a possible alteration of antioxidant pathways related to selenium metabolism but it does not present a direct evidence on selenoenzymes inhibition.

It was previously shown that citrate coated AgNP induced toxicity in RTgutGC cells targeting specifically the lysosomes (Minghetti and Schirmer, 2016) and that dissolved Ag is a potent disruptor of the homeostasis of essential trace elements such as zinc, iron and copper (Minghetti and Schirmer, 2019). Therefore, considering previous evidence of selenoenzyme inhibition (Srivastava et al., 2012), in this study, we evaluate the impact of both $AgNO_3$ and AgNP specifically on selenoprotein (GPx and TrxR) function via measurement of their mRNA levels and enzyme activity in RTgutGC cells. RTgutGC cells have been shown to be a relevant in vitro model of the rainbow trout (*Oncorhynchus mykiss*) intestine (Minghetti et al., 2017). Moreover, as selenoproteins inhibition might affect the cellular antioxidant machinery (Lu and Holmgren, 2009) the role of Ag and AgNP on oxidative stress was also evaluated. The effect of Ag on cellular oxidative stress was evaluated indirectly by determining the mRNA levels of glutathione reductase (GR) which was previously shown to be a good marker of oxidative stress (Minghetti et al., 2008) and directly by detection of reactive oxygen species (ROS) using a fluorescent probe, 2′,7′-dichlorodihydrofluorescein diacetate (H_2DCFDA). Moreover, intracellular bio-reactivity of Ag was also evaluated by measuring the Metallothionein b (MTb) mRNA levels, a known biomarker of metal exposure (Coyle et al., 2002; Minghetti et al., 2014) and by measuring nuclei surface area as Ag was recently shown to translocate to the cell nuclei in cells exposed to AgNP (Tardillo Suárez et al., 2020).

2. Materials and methods

2.1. Preparation of exposure solutions

Citrate coated AgNPs (cit-AgNP; nominal size: 19 nm, NanoSys GMbH, Switzerland) were purchased as aqueous suspension with a concentration of total Ag of 1 g/L (9.27 μM, pH 6.46). Cit-AgNP hydrodynamic diameter in water and in the exposure medium L-15/ex was previously measured at 40 nm and ~ 800 nm after 24 h by dynamic light scattering (DLS; Nano ZS, Malvern Instruments, Malvern, UK) with a zeta potential of − 28 mV and − 16 mV, respectively (Minghetti and Schirmer, 2019, 2016). The cit-AgNP characterization is also reported in Fig. S2. Silver nitrate stock solution was freshly prepared before each experiment at a concentration of 10 mM in ultrapure water (16–18 MΩ cm^{-1}; Gen pure, Thermo Scientific, USA). The exposure solutions were prepared as previously described (Minghetti and Schirmer, 2016). Briefly, solutions were prepared freshly by spiking the desired amounts of stock solutions into the exposure medium. Each solution was mixed thoroughly using a vortex mixer. The $AgNO_3$ and cit-AgNP solutions were prepared to contain identical nominal concentrations of total Ag, which were confirmed by ICP-OES measurement. The characterization of the same AgNP type has been previously reported and is summarized in Table S1 (Minghetti and Schirmer, 2016, 2019; Minghetti et al., 2019). RTgutGC cells were exposed in a minimal medium, L-15/ex (Schirmer et al., 1997). L-15/ex has an identical composition of Leibovitz's L-15 but without amino acids or vitamins thus avoiding scavenging of Ag^+ by amino acids or proteins (Minghetti and Schirmer, 2016). A side by side comparison of Ag toxicity and intracellular accumulation was conducted by exposing RTgutGC cells to 1 μM, 2 μM and 5 μM of $AgNO_3$ and cit-AgNP respectively, followed by incubation at 19 °C for 24 h in the dark. For evaluating gene expression, cells were exposed to $AgNO_3$ at 0.4 μM (non-toxic) and 1 μM (corresponding to the EC30 value) and to cit-AgNP at 0.4 μM and 1 μM, which are both non-toxic (Minghetti and Schirmer, 2016). For the oxidative stress study, cells were exposed to $AgNO_3$ at 0.4 μM (non-toxic), 1 μM (corresponding to EC30 value), 2 μM (corresponding to EC70 value) and 5 μM (corresponding to EC 90) and to cit-AgNP at 1 μM (non-toxic), 5 μM (corresponding to EC15 value) and 10 μM (corresponding to EC35 value) respectively. To evaluate the effect of $AgNO_3$ and cit-AgNP on the GPx and TrxR enzyme activity, RTgutGC cells were exposed to $AgNO_3$ at 0.4 μM (non-toxic) and 1 μM (corresponding to EC30 value) and to cit-AgNP at 1 μM (non-toxic) and 5 μM (corresponding to EC15 value) respectively. Non-toxic and toxic concentrations of $AgNO_3$ and cit-AgNP were calculated by averaging the alamarBlue and CFDA-AM cytotoxicity assay data previously reported (Minghetti and Schirmer, 2016).

2.2. RTgutGC cell culture

RTgutGC cells were cultured as previously described (Minghetti and Schirmer, 2016). The cells were routinely cultured in the commercial cell culture medium Leibovitz' L-15 (Gibco/Thermo Fisher Scientific, Waltham, MA, USA) supplemented with 5% fetal bovine serum (FBS; Sigma, USA) and 1% Gentamicin (L-15/FBS; Thermo Fisher Scientific, Waltham, MA, USA) in 75 cm^2 flasks (Greiner Bio-One, US) at 19 °C and split into two flasks once they reached approximately 80–90% confluency. For cell splitting, confluent flasks were washed twice with Versene (Thermo Fisher Scientific, Waltham, MA, USA) and cells were detached using 0.25% trypsin in phosphate buffer (PBS; Thermo Fisher Scientific, Waltham, MA, USA). When seeding cells for exposure experiments, cells were counted using an automated cell counter (Countess II automated cell counter, Thermo Fisher Scientific, Waltham, USA), and seeded at a concentration appropriate for the specific experiment.

2.3. Cell viability assay

Cytotoxicity in RTgutGC cells was evaluated in 24 multi-well plates (Greiner Bio-One, USA). The test plate contained three pseudo replicates of each exposure concentration, one blank well (without cells), three L-15/ex controls and two L-15/FBS controls. Both L-15/ex and L-15/FBS served as negative controls in the cytotoxicity assay. Cell viability assays were performed 4 times independently with cells of different passages.

RTgutGC cells were seeded in L-15/FBS complete media at a density of 74,000 cells/cm^2 and incubated at 19 °C for 48 h to allow attachment of the cells and development of a confluent monolayer on the multi-well plate surface. Following the incubation, the media was aspirated and cell monolayers were washed twice with L-15/ex and the exposure solutions 1 μM, 2 μM and 5 μM of $AgNO_3$ and cit-AgNP were applied. Cells were then incubated for 24 h. The exposure solution was aspirated from the wells and the cells were washed with L-15/ex. Following this, a 5% (v/v) alamarBlue (AB; Thermo Fisher Scientific, Waltham, MA, USA) and 4 μM of CFDA-AM (CFDA-AM; Thermo Fisher Scientific, Waltham, MA, USA) solution in L-15/ex was added to each well. AlamarBlue measures cell metabolic activity while CFDA-AM measures membrane integrity (Bloch et al., 2017; Minghetti and Schirmer, 2016). The plates were incubated in the dark at 19 °C for 30 min. Fluorescence was then recorded for both AB and CFDA-AM simultaneously with a Cytation 5 multi-well plate reader (Biotek, USA), at excitation/emission wavelengths of 530/595 nm and 485/530 nm for AB and CFDA-AM, respectively. After fluorescence reading, the AlamarBlue/CFDA-AM working solution was aspirated and a 1.5% (v/v, in L-15/ex) Neutral Red solution (NR; Sigma-Aldrich, St. Louis, MO, USA), an indicator of lysosome integrity, was added to the cells. Cells were incubated for 1 h in the dark at 19 °C. The Neutral Red solution was then aspirated, and the fixative solution (0.5% v/v formaldehyde and 1% w/v $CaCl_2$) was added, then aspirated after a few seconds. Finally, the extraction solution (1% v/v acetic acid and 50% v/v ethanol) was added and the plates were incubated with gentle horizontal agitation for 10 min in the dark at 19 °C. Afterwards, the fluorescence was recorded at excitation/emission wavelengths of 530/635 nm. Results obtained are reported as % viability based on fluorescent units (FU) of the L-15/ex control and calculated using following equation:

$$\% \text{ of control} = (FU_{\text{ex.cells}} - FU_{\text{ex.no cells}}) \times 100 / (\text{Average } [FU_{\text{con.}} - FU_{\text{con.no cells}}])$$

2.4. Determination of nuclear surface area

RTgutGC cells were seeded on TPP (Zellkultur und Labortechnologie, CH) flat bottom 96 well plates at a seeding density of 29,412 cells per cm^2 and incubated in the dark for 48 h. Afterwards, the cells were washed twice with 100 μL of L-15/ex and exposed for 24 h to 100 μL of L-15/ex medium alone (i.e. negative control) or supplemented with 0.1 μM, 0.4 μM, 0.8 μM, 1 μM, 2 μM, and 3 μM of $AgNO_3$ and 1 μM, 2 μM, 3 μM, 5 μM, and 10 μM of cit-AgNP solutions respectively. All exposures were prepared in triplicate (i.e. in three wells) and the experiment was repeated three times with cells of different passages. After exposure, 100 μL of the nuclear staining solution was added and cells were incubated in the dark for 30 min. The nuclear staining solution was prepared by adding 2 drops of NucBlue™ (Thermo Fisher Scientific, Waltham, MA, USA) for every mL of L-15/ex. Imaging was performed using the Cytation 5 plate reader equipped with Gen 5 software and using the 20× objective and the DAPI filter cube (Biotek, USA), at excitation/emission wavelengths of 377/447 nm. An area of 0.115 cm^2 was analyzed which is equal to 34% of the total surface area of each well. To prevent the incorporation of artefacts, minimum nuclei size of 5 μm in diameter was set on the software. The average nuclear surface area per cells was calculated by dividing the total nuclear surface by the number of nuclei using Gen 5 software (Biotek, USA). Bright field microscopic images were also collected using the 20× objective to evaluate possible morphological changes caused by exposure to $AgNO_3$ and cit-AgNP.

2.5. Quantification of intracellular silver

Quantification of intracellular Ag was performed as previously described (Minghetti and Schirmer, 2016). RTgutGC cells were seeded in 6 well plates at a density of 74,000 cells per cm^2 and incubated at 19 °C for 48 h. After, cells were washed with L-15/ex and exposed to 1 μM, 2 μM and 5 μM doses of $AgNO_3$ and cit-AgNP, respectively. An aliquot of the exposure media was collected for quantification of total Ag (Table S1). After exposure, the cells were washed twice with a 0.5 mM cysteine solution in PBS to remove loosely bound Ag. Cells were then lysed by adding 1 mL of 50 mM NaOH and incubated for 2 h in a shaker. An aliquot (100 μL) of the cell lysate was used for protein quantification using the modified Lowry assay (Thermo Fisher Scientific, Waltham, USA). The remaining 900 μL of the cell lysate was desiccated using a SpeedVac (Eppendorf, Germany). Samples were digested overnight by adding 800 μL of 69% HNO_3. 200 μL of H_2O_2 was added and incubated for at least one more hour, then the entire mixture was transferred quantitatively to a 15 mL falcon tube and diluted with ultrapure water bringing the concentration of acid to 5% HNO_3. Total Ag was determined by ICP-OES (iCAP 7400; Thermo Scientific, Waltham, MA, USA). Validation and calibration of the ICP-OES was achieved by using Ag reference standard (CPI International, Santa Rosa, CA, USA). Additionally, an in-line Yttrium internal standard (Peak Performance Inorganic Y Standard, CPI International, Santa Rosa, CA, USA) was used to correct for any instrument drift or matrix effects. Blanks, consisting of 5% HNO_3 in ultrapure water, were also run to correct for background levels.

2.6. RNA extraction, cDNA synthesis and determination of gene expression by qPCR

RTgutGC cells were seeded at a density of 74,000 cells /cm2 in 6 well plates for 48 h. The cells were washed with L-15/ex, then exposed to 0.4 μM and 1 μM of cit-AgNP and $AgNO_3$ prepared in L-15/ex. Then after 24 and 72 h of exposure, the exposure medium was removed and total RNA was extracted using TRIzol reagent (Invitrogen, USA) following manufacturer instructions. All samples were treated with TURBO DNA-free kit (Thermo Fisher Scientific, USA) to eliminate any traces of DNA. RNA quantity and quality were then determined by spectrophotometry using the Cytation 5 plate reader and RNA integrity by gel electrophoresis using 0.5 μg of total RNA in 1% agarose gel. Complementary DNA was synthesized using 1 μg of total RNA using the Maxima H Minus First Strand cDNA Synthesis Kit (Thermo Fisher Scientific, USA) following manual instructions. Messenger RNA levels of target genes (GPx, TrxR, MTb and GR) were measured by quantitative PCR (qPCR) using the SyBr Green iTaq Universal, (Bio-Rad, USA). Quantitative PCR conditions followed those suggested by Bio-Rad, except for MTb, where a 3 step program was applied, 95 °C for 5 s, 55 °C for 30 s and 72 °C for 30 s. The PCR efficiency of each reaction was above 95%. Absolute copy number quantification was achieved by running a parallel set of reactions containing standards consisting of a serial dilution of linearized plasmid containing the target gene and were automatically calculated using the Bio-rad software (CFX Manager™ 3.0). The method used to generate the plasmid containing target genes is reported in the Supplementary information. Messenger RNA levels were reported as the fold change of the gene copy numbers in the treated from the untreated sample. The gene copy numbers were reported in Fig. S1. Normalization was based on the geometric mean expression of two reference genes (ubiquitin and elongation factor 1α) as previously described (Minghetti and Schirmer, 2016).

2.7. GPx and TrxR enzyme activity assays

RTgutGC cells were seeded at a density of 80,000 cells/cm^2 in 75 cm^2 flasks (Greiner Bio-One, US) and incubated at 19 °C for 6 days. After, the cell monolayers were washed with L-15/ex and exposed to non-toxic (0.4 μM of $AgNO_3$ and 1 μM of cit-AgNP) and toxic (1 μM of $AgNO_3$ and 5 μM of cit-AgNP) doses for 24 h. Following exposure, cells were washed with L-15/ex and then collected using a cell scraper and transferred into a 15 mL tube. The cells were centrifuged at 1000×*g* for 10 min and homogenized in enzyme assay buffer (50 mM Tris-HCl, pH 7.6,

containing 5 mM EDTA) using an ultrasonic homogenizer (Vibra-Cell™ Ultrasonic Liquid Processors, Sonics and Materials Inc., CT, USA). The cell lysate was centrifuged again at 10,000×*g* for 15 min at 4 °C to obtain a supernatant containing the cytoplasmic proteins which were separated from pellet containing the membrane-bound proteins. The enzymatic activity was then measured from a 20 μL aliquot by following the manual instructions in the assay kit (Glutathione peroxidase and Thioredoxin reductase assay, Cayman chemicals, MI, USA). The GPx activity was based on the oxidation of NADPH (Nicotinamide adenine dinucleotide phosphate) to $NADP^+$ that is accompanied by a decrease in absorbance at 340 nm which is directly proportional to the GPx activity of the sample. While TrxR activity was based on the reduction of DTNB (5,5′-dithiobis-(2-nitrobenzoic acid), Ellman's reagent) with NADPH to TNB (2-nitro-5-thiobenzoate). TrxR activity was measured spectrophotometrically at 405 nm. An aliquot (100 μL) of the cell lysate was used for protein quantification using the modified Lowry assay (Thermo Scientific, Waltham, MA). The enzymatic activity was normalized by the total protein content and reported as nmol/min/mg of protein for GPx activity and μmol/min/mg of protein for TrxR activity, respectively.

2.8. Detection of reactive oxygen species

RTgutGC cells were seeded at a density of 31,000 cells/ cm^2 in 96-well TPP flat bottom plates (Greiner Bio-One, US Bio-One, US Bio-One, US). After 48 h, cells were exposed to 0.4 μM, 1 μM, 2 μM and 5 μM of $AgNO_3$, or 1 μM, 5 μM and 10 μM of cit-AgNP. H_2O_2 was used as a positive control at 6% (w/w) (2.00 mM; Fig. S3). All exposure solutions were prepared in L-15/ex. Each experiment included at least three pseudo replicates and was repeated 3 times with cells of different passages. The exposure time points were 1 h, 5 h and 24 h. At each time point, the cells were washed with L-15/ex and then incubated with 5 μM of 2′,7′-dichlorodihydrofluorescein diacetate (H_2DCFDA; Thermo Fisher Scientific, USA) dye in L-15/ex for 30 min. Finally, the cells were washed gently with L-15/ex and read using the Cytation-5 plate reader at absorbance/emission wavelength of 485/520 nm. The H_2DCFDA dye was used to detect the presence of ROS in cells.

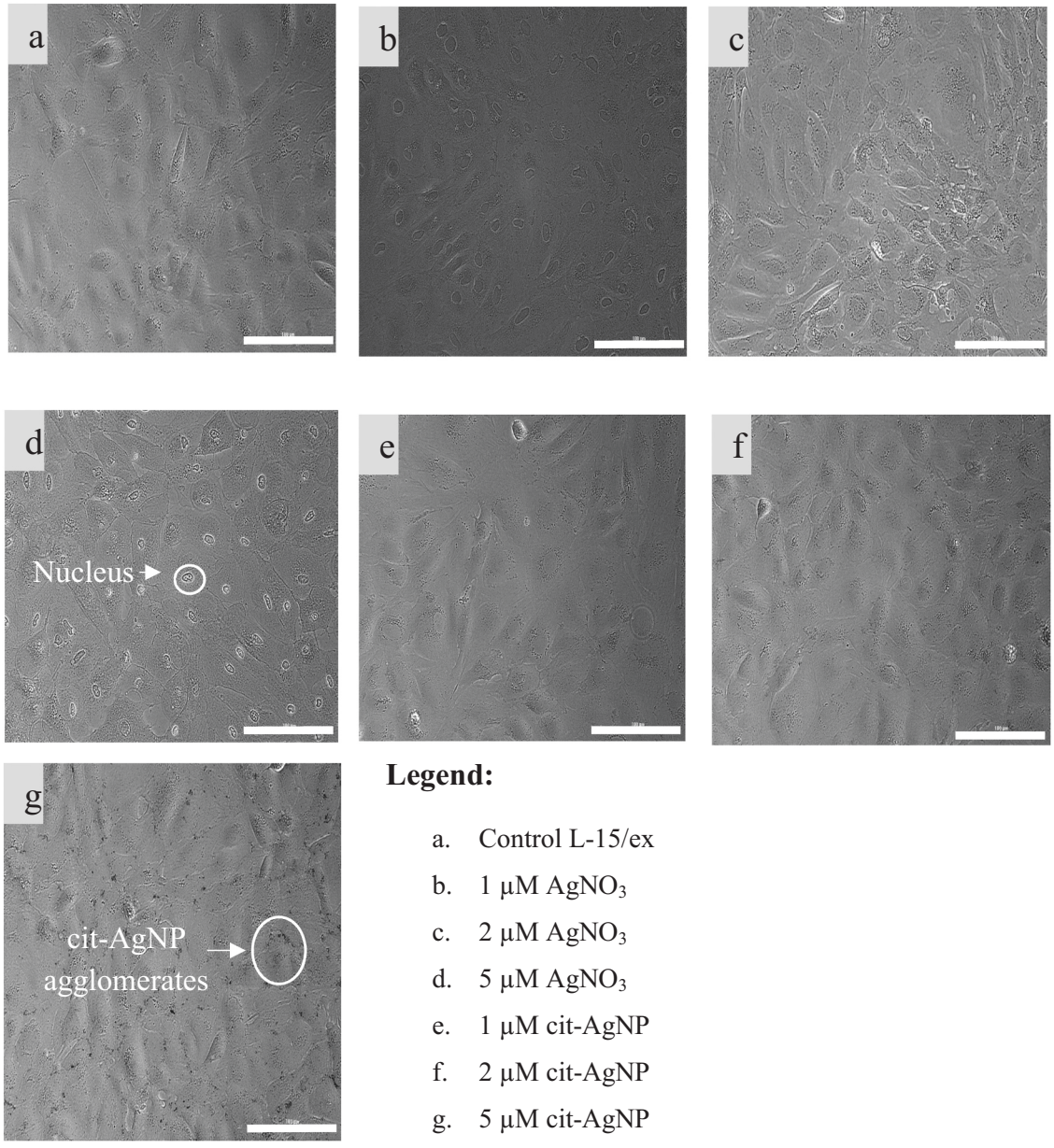

Fig. 1. Bright field images of RTgutGC cells exposed to $AgNO_3$ and cit-AgNP for 24 h. Reduction in nuclei size was observed in cells exposed to 5 μM of $AgNO_3$ and is indicated by a white circle in (d); cit-AgNP agglomerates was observed on cells (g). Scale bars = 100 μm.

2.9. Data analysis

Statistical analysis was performed using GraphPad Prism Version 8.0 (GraphPad Software Inc., San Diego, CA). For multiple groups, statistical analysis was performed by the analysis of variance (ANOVA) followed by Tukey's post hoc test for comparison of multiple groups or Dunnett's post hoc test when comparing to a control group. Values of $p < 0.05$ were considered statistically significant.

3. Results

3.1. Cytotoxicity of cit-AgNP and $AgNO_3$

Following exposure, bright field microscopic images were collected to evaluate possible morphological changes caused by exposure to $AgNO_3$ and cit-AgNP (Fig. 1). Reduction in nuclei size was visually observed in cells exposed to 5 μM of $AgNO_3$ only (Fig. 1d). While accumulation and agglomeration of nanoparticles was observed on top of cells exposed to 5 μM of cit-AgNP (Fig. 1g). The effect of Ag on cell nuclei size was further quantified using an automated imaging analysis method (Fig. 2). A 17%, 18%, 15% and 18.5% decrease in the nuclear surface area was observed in cells exposed to toxic concentrations of 0.8 μM, 1 μM, 2 μM and 3 μM of $AgNO_3$, respectively. Conversely, no significant decrease in nuclear surface area was observed in cells exposed to cit-AgNP. Exposure to $AgNO_3$ induced toxicity in RTgutGC in a dosed-dependent manner. However, $AgNO_3$ was more toxic than cit-AgNP. This is shown by the exposure to 5 μM of $AgNO_3$ or cit-AgNP which resulted in a ~ 80% or ~ 20% reduction in cell viability, respectively (Fig. 3A).

3.2. Intracellular silver accumulation

RTgutGC cells were exposed to identical concentrations of $AgNO_3$ or cit-AgNP at 1 μM, 2 μM and 5 μM for 24 h in order to evaluate the intracellular accumulation of total Ag. Cells exposed to equimolar amount of $AgNO_3$ or cit-AgNP accumulated the same amounts of Ag intracellularly (Fig. 3B).

3.3. Messenger RNA levels of target selenoprotein genes and other biomarkers

At 24 h of exposure, only the highest doses of $AgNO_3$ and cit-AgNP (1 μM) induced a significant increase of MTb levels (13.67 ± 7.07 and 10.43 ± 5.62-fold increase), whereas all other tested genes showed no alteration of their mRNA levels when compared to control (Fig. 4). After 72 h exposure, MTb mRNA levels were reduced back to control levels in cells exposed to 1 μM $AgNO_3$ and cit-AgNP. All other genes in cells exposed for 72 h showed mRNA levels not statistically different from

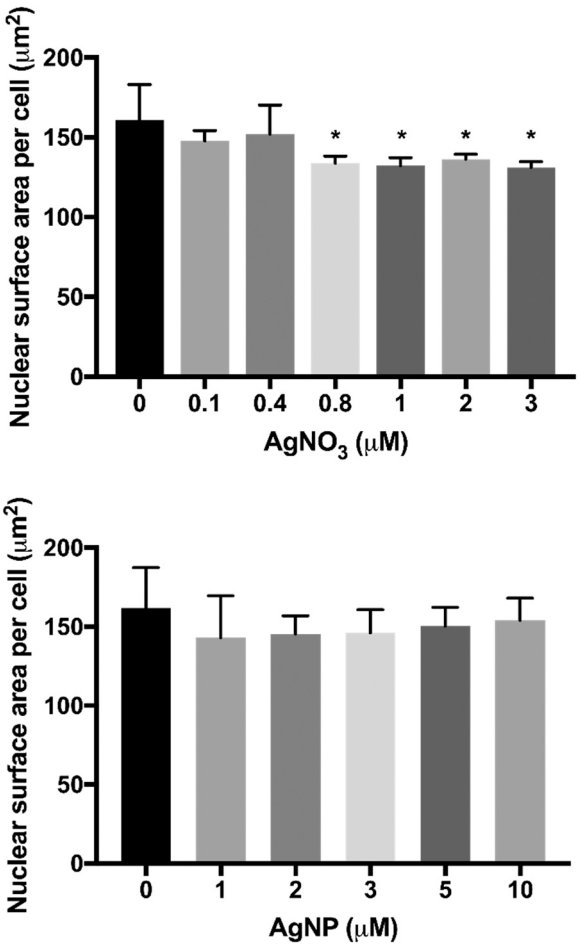

Fig. 2. Measurement of nuclear surface area in RTgutGC cells exposed to $AgNO_3$, and cit-AgNP for 24 h. Values are mean ± standard deviation of 3 independent experiments n = 3. Statistical difference from respective control, i.e. untreated cells at each time point is indicated by an asterisk (One-way ANOVA, Dunnett's Test, $p < 0.05$).

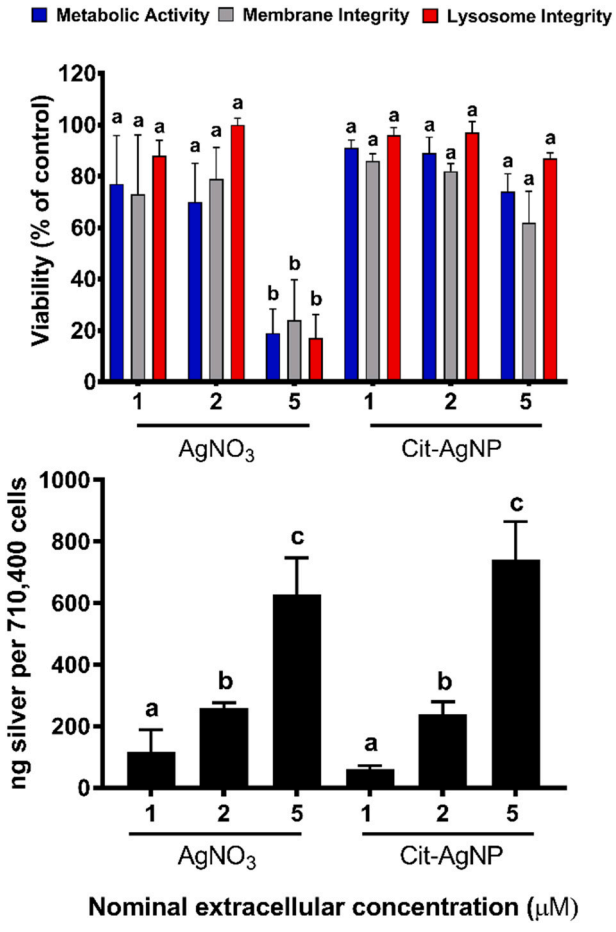

Fig. 3. A) Cytotoxicity of $AgNO_3$ and cit-AgNP in RTgutGC after 24 h of exposure. Metabolic activity was measured using alamarBlue assay, membrane integrity was measured by CFDA-AM assay and lysosome integrity was measured by Neutral Red assay. Values are mean ± standard deviation, n = 4. Significant differences are indicated by different lettering (One-way ANOVA, Tukey's post hoc test, $p < 0.05$). B) Intracellular Ag accumulation in cells exposed to equimolar concentrations of $AgNO_3$ and cit-AgNPs for 24 h. Values are means ± SD, n = 3 (One-way ANOVA, Tukey's post hoc test, $p < 0.05$).

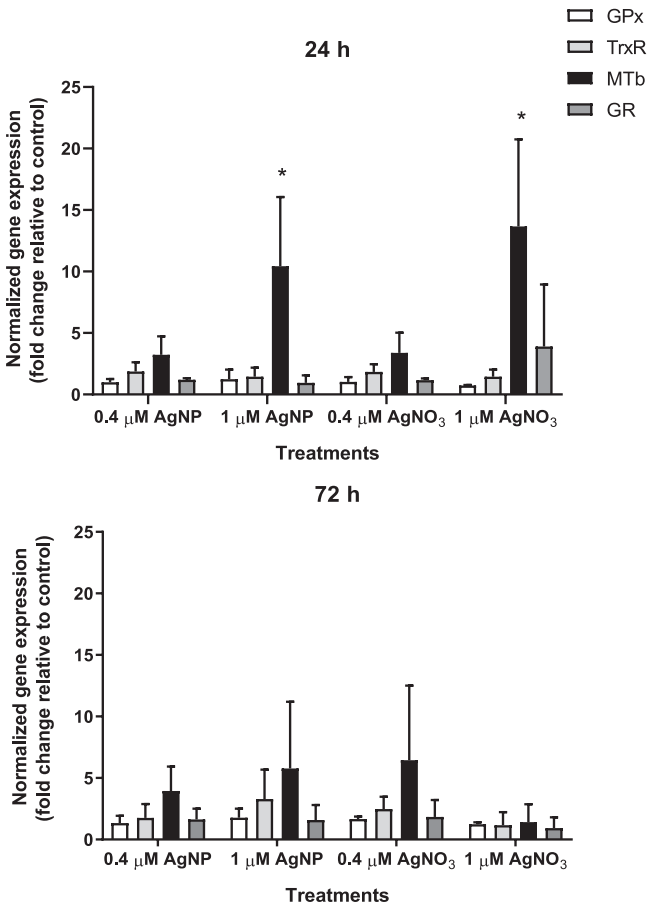

Fig. 4. Normalized mRNA levels of GPx, TrxR, GR and MTb genes measured in RTgutGC cells exposed to $AgNO_3$ and cit-AgNP for 24 h. Target genes normalized expression is reported as ratio of the expression in cells exposed to control media L-15/ex (Fig. S1). Values represent mean normalized fold change ± standard deviation, n = 3–5. Statistical difference from respective control, i.e. untreated cells at each time point is indicated by an asterisk (One-way ANOVA, Dunnett's Test, $p < 0.05$).

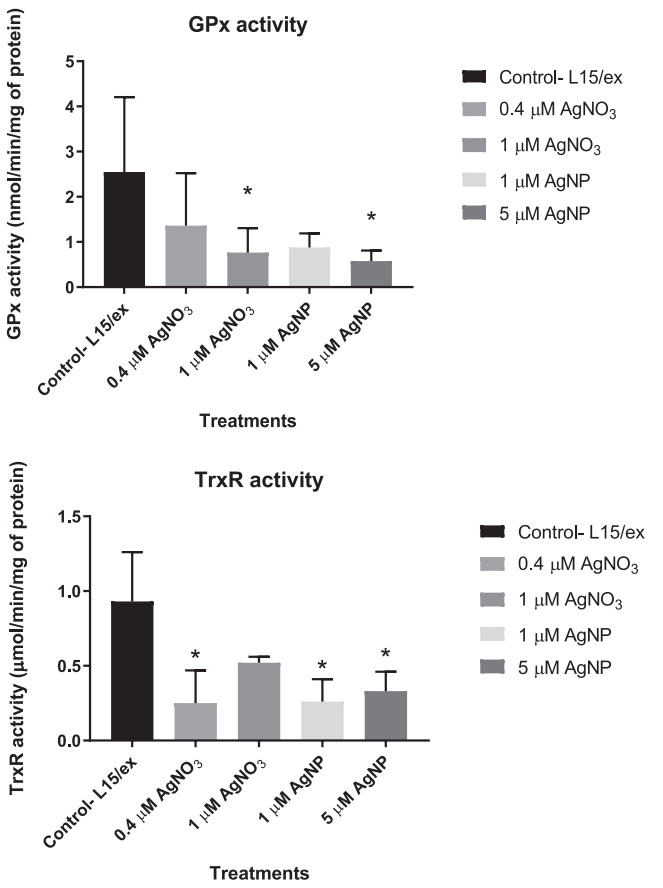

Fig. 5. GPx and TrxR enzymatic activity measured in RTgutGC cells exposed to $AgNO_3$ and cit-AgNP for 24 h. The enzyme activity values were normalized per mg of total protein. Values are mean ± standard deviation, n = 3. Statistical difference from respective control, i.e. untreated cells at each time point is indicated by an asterisk (One-way ANOVA, Dunnett's Test, $p < 0.05$).

control (Fig. 4).

3.4. Activity of selenoenzymes in response to toxic and non-toxic concentrations of $AgNO_3$ and cit-AgNP

Exposure to toxic concentrations of $AgNO_3$ (1 μM) and cit-AgNP (5 μM) induced a decrease of about 50% and 60% in the GPx enzyme activity when compared to the control, respectively. There was no significant difference in the GPx activity in samples exposed to non-toxic $AgNO_3$ and cit-AgNP concentrations (0.4 μM $AgNO_3$ and 1 μM cit-AgNP). Moreover, exposure to 0.4 μM $AgNO_3$, 1 μM cit-AgNP and 5 μM of cit-AgNP induced a reduction of ~ 50%, 35% and 30% in TrxR activity compared to control, respectively (Fig. 5).

3.5. Oxidative stress induction by $AgNO_3$ and cit-AgNP over time

Oxidative stress in RTgutGC cells exposed to increasing doses of $AgNO_3$ (0.4 μM, 1 μM, 2 μM and 5 μM) and cit-AgNP (1 μM, 5 μM and 10 μM) is reported in Fig. 6. None of the treatments resulted in a variation in reactive oxygen species in RTgutGC cells, not even the 2 mM H_2O_2 exposure. However, 2 mM H_2O_2 dissolved in the exposure medium (L-15/ex), in absence of cells, resulted a sharp increase in relative fluorescence intensity in absence of cells. None of the other treatment induced or reduced the fluorescence of H_2DCFDA in solution (Fig. S3).

4. Discussion

In this study, we show that dissolved and nano Ag can inhibit selenoenzymes activity (GPx and TrxR) in fish intestinal cells (RTgutGC). This finding supports previous data obtained in mammalian systems (Gmoshinski et al., 2016; Srivastava et al., 2012). On the other hand, no significant effects were observed on selenoproteins at the mRNA levels and on oxidative stress. Silver nitrate and cit-AgNP were shown to bioaccumulate in a similar manner in RTgutGC cells. This is in line with previous in vivo and in vitro studies (Clark et al., 2019a; Minghetti et al., 2019). However, equimolar amounts of intracellular $AgNO_3$ were found to be more toxic than cit-AgNP here as well as in several other studies (Minghetti and Schirmer, 2019; Miura and Shinohara, 2009; Yue et al., 2017). Given that cit-AgNP was shown to remain mostly in nano form for up to 72 h in RTgutGC cells (Minghetti et al., 2019), and considering our toxicity data, we can hypothesize that Ag ions but not AgNP are the major contributors of toxic effects in the cell.

In our study we have also observed that dissolved Ag toxicity results in a decrease in cell nucleus size. Several other studies have shown that $AgNO_3$ induces apoptosis in cells causing nuclear condensation and fragmentation (Foldbjerg et al., 2009; Kaplan et al., 2017). Kaplan et al. (2017) revealed that $AgNO_3$ induced apoptosis by increasing the levels of ROS in mammalian cells- HaCat and K562 erythroleukemia cells and that a change in nuclear surface area was confirmed by condensed chromatin (Kaplan et al., 2017). Moreover, in HeLa cells, $AgNO_3$ and AgNP induce apoptosis and this effect was associated with the induction of Metallothionein (MT-2A) and other genes such as heme oxygenase and heat shock proteins (Miura and Shinohara, 2009). Similarly, in

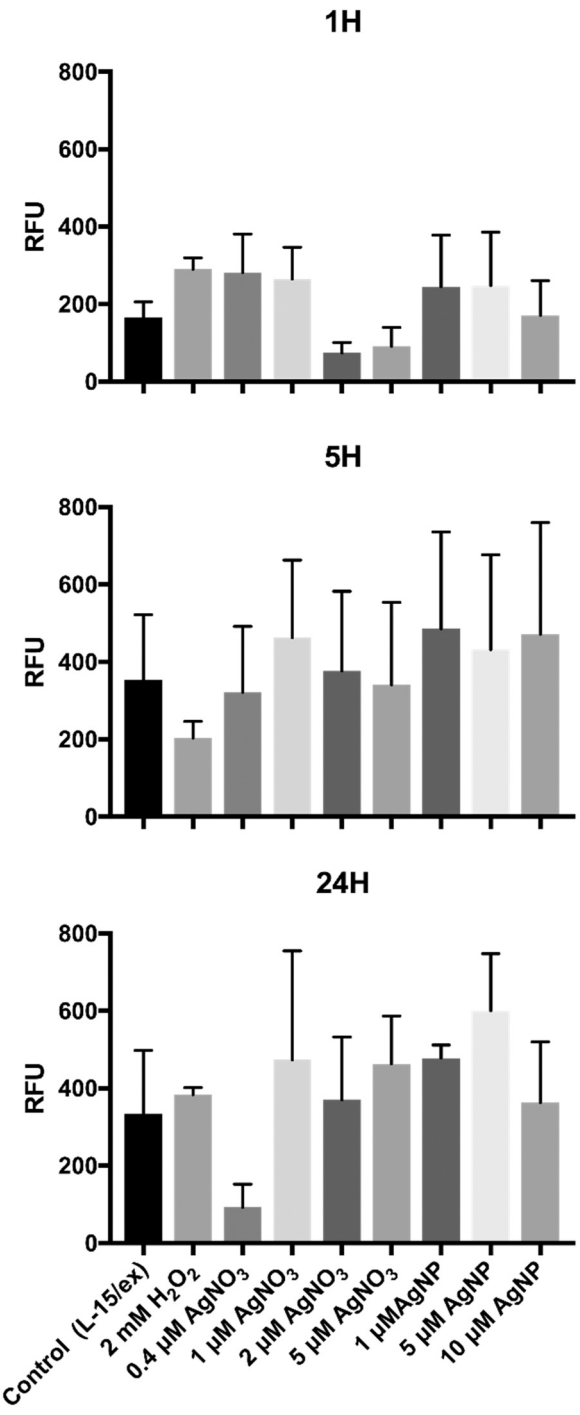

Fig. 6. Determination of ROS in RTgutGC cells exposed to $AgNO_3$ and cit-AgNP at 1 h, 5 h and 24 h. 2 mM H_2O_2 was used as positive control (see Fig. S3). ROS were detected using the H_2DCFDA assay. The data is reported in relative fluorescent unit (RFU). Values are means ± standard deviation of four independent experiments, n = 4. No difference from controls was found (1-way ANOVA, Dunnett's test, $p < 0.05$).

RTgutGC it was shown that $AgNO_3$ and cit-AgNP induce MTb an effect shown repeatedly in RTgutGC cells (Minghetti and Schirmer, 2019, 2016). Although in this study we did not measure specific biomarkers of apoptosis, our data supports the above-mentioned studies and suggest that the reduction in cell nucleus size might be an indication of apoptosis induced by dissolved Ag.

Glutathione (GSH) and its associated enzymes, GPx and TrxR, are controlled by the nuclear factor-2 related erythroid factor-2 (Nrf2) transcription factor (Li et al., 2016; Tindell et al., 2018). It was shown that AgNP induced an oxidative stress response mediated by a Nrf2/heme oxygenease-1 signaling pathways (Aueviriyavit et al., 2014; Polet et al., 2020) and that Nrf2 has a protective role against DNA damage and apoptosis induced by AgNP (Kang et al., 2012). However, it should be noted that in these studies cells were exposed to concentrations of AgNP much higher than in our study (46–139 µM). Furthermore, it was shown in several cell lines that the activation of Nrf2 requires a concentration of at least 2.5 µM of dissolved Ag (silver chloride) and that the high level of intracellular glutathione in these cell lines provided protection from oxidative stress at lower exposure concentration (Simmons et al., 2011). In our study, mRNA levels of GPx, TrxR and GR were not induced after exposure to $AgNO_3$ and cit-AgNP at lower concentrations (0.4–1 µM) indicating that this concentration might be too low to induce Nrf2 target genes (Polet et al., 2020; Simmons et al., 2011; Sun et al., 2017).

Metals with multiple oxidation states like iron, copper, cobalt and nickel have been shown to take part in the Fenton reaction by converting hydrogen peroxide, produced in cells, to hydroxyl radicals ($^{\bullet}OH$) (Rubino, 2015). For example, copper (+ 1 to + 2) and iron (+ 2 to + 3) cycle between two oxidation states and undergo two-electron redox chemistry in the cells. Conversely, the non-essential metal Ag maintain a stable oxidation state of + 1 and is not able to take part in the Fenton reaction (Font et al., 2014). Therefore, Ag is not directly inducing ROS formation via the Fenton reaction. In our experiment, exposure to $AgNO_3$ or cit-AgNP did not result in the direct measurement of ROS or induction of GR mRNA levels in RTgutGC cells which could be explained by Ag oxidation state. Similarly, in Caco-2 cells no ROS induction was found in cells exposed up to 1.15 mM of AgNP (Aueviriyavit et al., 2014). Moreover, the induction of MTb by 1 µM of $AgNO_3$ and AgNP in RTgutGC might be involved in intracellular Ag scavenging and protect the cell against oxidative stress. Therefore, our results together with previous studies mentioned above suggest that Ag is not directly inducing oxidative stress in intestinal cells and might induce toxicity via a different mechanism of toxic.

In RTgutGC the main toxic effect measured in this study was the inhibition of GPx and TrxR enzyme activity. The possible mechanism behind the disruption of selenoenzyme activity by Ag could be explained by its affinity for the thiol group of proteins which could interfere with the seleno-cysteine-rich domain of proteins (Srivastava et al., 2012). Selenocysteine is an amino acid analogous to cysteine containing a selenol group in place of the sulfur-containing thiol group in cysteine (Turanov et al., 2011). Hence, a metal with high affinity for the thiol group such as Ag can directly displace Se from the selenocysteine domain leading to inhibition of selenoenzyme function (Behra et al., 2013; Liu et al., 2017). Thus, the GPx and TrxR enzyme inhibition, suggests that the main mechanism of toxic action of Ag is the binding of Ag to the thiol group of proteins which alters the function of enzymes, a mechanism previously described (Rubino, 2015). A similar effect, has been observed in mammals exposed to dissolved metals such as mercury, cadmium, arsenic and lead due to their chemical affinity for thiol groups (i.e. selenocysteine) (Rubino, 2015) which suggest that metals directly affect selenoenzymes activity but do not induce direct transcriptional regulation, at least not at relatively low exposure concentrations (~ 1 µM).

Selenium is an important component of fish nutrition as it is necessary for normal fish growth and proper physiological and biochemical functions (Khan et al., 2017). Any disturbance in the Se homeostasis (deficiency and excess) can result in an impaired antioxidant activity leading to susceptibility of fish to oxidative stress and a reduction in growth and survival (Gao et al., 2019). Recently, AgNP have been shown to be a potent antimicrobial and antiparasitic agent and have been tested as an alternative product in aquaculture (Bravo-Guerra et al., 2020; Fuentes-Valencia et al., 2020; Swain et al., 2014). Although initial studies show that AgNP are effective against bacteria and protozoan parasites at concentrations that are not acutely toxic to fish (i.e. up to

927 μM) (Bravo-Guerra et al., 2020; Clark et al., 2019a; Fuentes-Valencia et al., 2020; Swain et al., 2014), chronic effects of exposure to AgNP should be investigated especially considering its interference with essential trace metal metabolism (Minghetti and Schirmer, 2019).

5. Conclusion

Our study establishes a clear pattern of the detrimental effects of acute $AgNO_3$ and cit-AgNP exposure including reduced cell viability and inhibition of selenoproteins TrxR and GPx in fish intestinal cells. Moreover, we show that $AgNO_3$ is more toxic than cit-AgNP at equimolar intracellular concentrations. However, the effect of chronic exposure in fish are not well understood. Future studies should focus on the consequences of chronic exposures of $AgNO_3$ and AgNP. For instance, use of lower concentrations, similar to the one shown to induce enzyme alterations in our study in vitro, and chronic exposures would bring a more environmentally relevant understanding of dissolved and nano- Ag. Overall, our study corroborates the role of Ag as a disruptor of essential trace elements which should be considered when weighing the beneficial and adverse effects of incorporating Ag in commercial products targeted for farmed animals and human consumption.

CRediT authorship contribution statement

Debarati Chanda: Conceptualization, Methodology, Writing - original draft. **William Dudefoi**: Investigation, Writing - review & editing. **Joshua Anadu**: Investigation. **Matteo Minghetti:** Writing - review & editing, Supervision, Project administration, Funding acquisition.

Declaration of Competing Interest

The authors declare that they have no known competing financial interests or personal relationships that could have appeared to influence the work reported in this paper.

Acknowledgments

This research was supported by the U.S. National Science Foundation (NSF) through award no. CBET-1706093 (M. M.).

Appendix A. Supporting information

Supplementary data associated with this article can be found in the online version at doi:10.1016/j.ecoenv.2021.111930.

References

Aueviriyavit, S., Phummiratch, D., Maniratanachote, R., 2014. Mechanistic study on the biological effects of silver and gold nanoparticles in Caco-2 cells - induction of the Nrf2/HO-1 pathway by high concentrations of silver nanoparticles. Toxicol. Lett. 224, 73–83. https://doi.org/10.1016/j.toxlet.2013.09.020.

Barros, D., Pradhan, A., Mendes, V.M., Manadas, B., Santos, P.M., Pascoal, C., Cássio, F., 2019. Proteomics and antioxidant enzymes reveal different mechanisms of toxicity induced by ionic and nanoparticulate silver in bacteria. Environ. Sci. Nano 6, 1207–1218. https://doi.org/10.1039/c8en01067f.

Behra, R., Sigg, L., Clift, M.J.D., Herzog, F., Minghetti, M., Johnston, B., Petri-Fink, A., Rothen-Rutishauser, B., 2013. Bioavailability of silver nanoparticles and ions: from a chemical and biochemical perspective. J. R. Soc. Interface 10, 20130396. https://doi.org/10.1098/rsif.2013.0396.

Bloch, S.R., Kim, J.J., Pham, P.H., Hodson, P.V., Lee, L.E.J., Bols, N.C., 2017. Responses of an American eel brain endothelial-like cell line to selenium deprivation and to selenite, selenate, and selenomethionine additions in different exposure media. Vitr. Cell. Dev. Biol. - Anim. 53, 940–953. https://doi.org/10.1007/s11626-017-0196-4.

Bravo-Guerra, C., Cáceres-Martínez, J., Vásquez-Yeomans, R., Pestryakov, A., Bogdanchikova, N., 2020. Lethal effects of silver nanoparticles on Perkinsus marinus, a protozoan oyster parasite. J. Invertebr. Pathol. 169, 107304 https://doi.org/10.1016/j.jip.2019.107304.

Bruneau, A., Turcotte, P., Pilote, M., Gagné, F., Gagnon, C., 2016. Fate of silver nanoparticles in wastewater and immunotoxic effects on rainbow trout. Aquat. Toxicol. 174, 70–81. https://doi.org/10.1016/j.aquatox.2016.02.013.

Burk, R.F., Hill, K.E., 2005. Selenoprotein P: an extracellular protein with unique physical characteristics and a role in selenium homeostasis. Annu. Rev. Nutr. 25, 215–235. https://doi.org/10.1146/annurev.nutr.24.012003.132120.

Cáceres-Saez, I., Haro, D., Blank, O., Aguayo-Lobo, A., Dougnac, C., Arredondo, C., Cappozzo, H.L., Ribeiro Guevara, S., 2019. Stranded false killer whales, Pseudorca crassidens, in Southern South America reveal potentially dangerous silver concentrations. Mar. Pollut. Bull. 145, 325–333. https://doi.org/10.1016/j.marpolbul.2019.05.047.

Clark, N.J., Boyle, D., Eynon, B.P., Handy, R.D., 2019a. Dietary exposure to silver nitrate compared to two forms of silver nanoparticles in rainbow trout: bioaccumulation potential with minimal physiological effects. Environ. Sci. Nano 6, 1393–1405. https://doi.org/10.1039/c9en00261h.

Clark, N.J., Boyle, D., Handy, R.D., 2019b. An assessment of the dietary bioavailability of silver nanomaterials in rainbow trout using an ex vivo gut sac technique. Environ. Sci. Nano 6, 646–660. https://doi.org/10.1039/C8EN00981C.

Coyle, P., Philcox, J.C., Carey, L.C., Rofe, A.M., 2002. Metallothionein: the multipurpose protein. Cell. Mol. Life Sci. 59, 627–647. https://doi.org/10.1007/s00018-002-8454-2.

Evans, D.H., 2008. Teleost fish osmoregulation: what have we learned since August Krogh, Homer Smith, and Ancel Keys. Am. J. Physiol. - Regul. Integr. Comp. Physiol. 295, 704–713. https://doi.org/10.1152/ajpregu.90337.2008.

Farkas, J., Christian, P., Gallego-Urrea, J.A., Roos, N., Hassellöv, M., Tollefsen, K.E., Thomas, K.V., 2011. Uptake and effects of manufactured silver nanoparticles in rainbow trout (Oncorhynchus mykiss) gill cells. Aquat. Toxicol. 101, 117–125. https://doi.org/10.1016/j.aquatox.2010.09.010.

Foldbjerg, R., Olesen, P., Hougaard, M., Dang, D.A., Hoffmann, H.J., Autrup, H., 2009. PVP-coated silver nanoparticles and silver ions induce reactive oxygen species, apoptosis and necrosis in THP-1 monocytes. Toxicol. Lett. 190, 156–162. https://doi.org/10.1016/j.toxlet.2009.07.009.

Font, M., Acuña-Parés, F., Parella, T., Serra, J., Luis, J.M., Lloret-Fillol, J., Costas, M., Ribas, X., 2014. Direct observation of two-electron Ag(I)/Ag(III) redox cycles in coupling catalysis. Nat. Commun. 5, 1–10. https://doi.org/10.1038/ncomms5373.

Fuentes-Valencia, M.A., Fajer-Ávila, E.J., Chávez-Sánchez, M.C., Martínez-Palacios, C.A., Martínez-Chávez, C.C., Junqueira-Machado, G., Lara, H.H., Raggi, L., Gómez-Gil, B., Pestryakov, A.A., Bogdanchikova, N., 2020. Silver nanoparticles are lethal to the ciliate model Tetrahymena and safe to the pike silverside Chirostoma estor. Exp. Parasitol. 209, 107825 https://doi.org/10.1016/j.exppara.2019.107825.

Gao, X. jiao, Tang, B., Liang, H. huang, Yi, L., Wei, Z. gong, 2019. Selenium deficiency induced an inflammatory response by the HSP60 - TLR2-MAPKs signalling pathway in the liver of carp. Fish Shellfish Immunol. 87, 688–694. https://doi.org/10.1016/j.fsi.2019.02.017.

Gmoshinski, I.V., Shumakova, A.A., Shipelin, V.A., Maltsev, G.Y., Khotimchenko, S.A., 2016. Influence of orally introduced silver nanoparticles on content of essential and toxic trace elements in organism. Nanotechnol. Russ. 11, 646–652. https://doi.org/10.1134/S1995078016050074.

Habas, K., Shang, L., 2019. Silver nanoparticle-mediated cellular responses in human keratinocyte cell line HaCaT in vitro. Nanoscale Rep. 2, 1–9. https://doi.org/10.26524/nr1921.

Jiang, H.S., Yin, L., Ren, N.N., Xian, L., Zhao, S., Li, W., Gontero, B., 2017. The effect of chronic silver nanoparticles on aquatic system in microcosms. Environ. Pollut. 223, 395–402. https://doi.org/10.1016/j.envpol.2017.01.036.

Kang, S.J., Ryoo, I. geun, Lee, Y.J., Kwak, M.K., 2012. Role of the Nrf2-heme oxygenase-1 pathway in silver nanoparticle-mediated cytotoxicity. Toxicol. Appl. Pharm. 258, 89–98. https://doi.org/10.1016/j.taap.2011.10.011.

Kaplan, A., Akalin Ciftci, G., Kutlu, H.M., 2017. The apoptotic and genomic studies on A549 cell line induced by silver nitrate. Tumor Biol. 39. https://doi.org/10.1177/1010428317695033.

Khan, A.M., Korzeniowska, B., Gorshkov, V., Tahir, M., Schrøder, H., Skytte, L., Rasmussen, K.L., Khandige, S., Møller-Jensen, J., Kjeldsen, F., 2019. Silver nanoparticle-induced expression of proteins related to oxidative stress and neurodegeneration in an in vitro human blood-brain barrier model. Nanotoxicology 13, 221–239. https://doi.org/10.1080/17435390.2018.1540728.

Khan, K.U., Zuberi, A., Fernandes, J.B.K., Ullah, I., Sarwar, H., 2017. An overview of the ongoing insights in selenium research and its role in fish nutrition and fish health. Fish Physiol. Biochem. 1–17. https://doi.org/10.1007/s10695-017-0402-z.

Labunskyy, V.M., Hatfield, D.L., Gladyshev, V.N., 2014. Selenoproteins: molecular pathways and physiological roles. Physiol. Rev. 94, 739–777. https://doi.org/10.1152/physrev.00039.2013.

Lemire, J.A., Harrison, J.J., Turner, R.J., 2013. Antimicrobial activity of metals: mechanisms, molecular targets and applications. Nat. Rev. Microbiol. 11, 371–384. https://doi.org/10.1038/nrmicro3028.

Li, Q., Wall, S.B., Ren, C., Velten, M., Hill, C.L., Locy, M.L., Rogers, L.K., Tipple, T.E., 2016. Thioredoxin reductase inhibition attenuates neonatal hyperoxic lung injury and enhances nuclear factor E2-related factor 2 activation. Am. J. Respir. Cell Mol. Biol. 55, 419–428. https://doi.org/10.1165/rcmb.2015-0228OC.

Liu, W., Worms, I.A.M., Herlin-Boime, N., Truffier-Boutry, D., Michaud-Soret, I., Mintz, E., Vidaud, C., Rollin-Genetet, F., 2017. Interaction of silver nanoparticles with metallothionein and ceruloplasmin: impact on metal substitution by Ag(i), corona formation and enzymatic activity. Nanoscale 9, 6581–6594. https://doi.org/10.1039/c7nr01075c.

Lu, J., Holmgren, A., 2009. Selenoproteins. J. Biol. Chem. 284, 723–727. https://doi.org/10.1074/jbc.R800045200.

Minghetti, M., Schirmer, K., 2016. Effect of media composition on bioavailability and toxicity of silver and silver nanoparticles in fish intestinal cells (RTgutGC). Nanotoxicology 10, 1526–1534. https://doi.org/10.1080/17435390.2016.1241908.

Minghetti, M., Schirmer, K., 2019. Interference of silver nanoparticles with essential metal homeostasis in a novel enterohepatic fish: in vitro system. Environ. Sci. Nano 6, 1777–1790. https://doi.org/10.1039/c9en00310j.

Minghetti, M., Leaver, M.J., Carpenè, E., George, S.G., 2008. Copper transporter 1, metallothionein and glutathione reductase genes are differentially expressed in tissues of sea bream (Sparus aurata) after exposure to dietary or waterborne copper. Comp. Biochem. Physiol. - C Toxicol. Pharmacol. https://doi.org/10.1016/j.cbpc.2008.01.014.

Minghetti, M., Schnell, S., Chadwick, M.A., Hogstrand, C., Bury, N.R., 2014. A primary FIsh Gill Cell System (FIGCS) for environmental monitoring of river waters. Aquat. Toxicol. 154, 184–192. https://doi.org/10.1016/j.aquatox.2014.05.019.

Minghetti, M., Drieschner, C., Bramaz, N., Schug, H., Schirmer, K., Minghetti, M., Drieschner, C., Bramaz, N., Schug, H., Schirmer Eawag, K., Drieschner, C., Schirmer, K., 2017. A fish intestinal epithelial barrier model established from the rainbow trout (Oncorhynchus mykiss) cell line, RTgutGC. Cell Biol. Toxicol. 33, 539–555. https://doi.org/10.1007/s10565-017-9385-x.

Minghetti, M., Dudefoi, W., Catalano, J.G., 2019. Environmental Science Nano Emerging Investigator Series: Linking Chemical Transformations of Silver and Silver Nanoparticles to their Bio-reactivity. https://doi.org/10.1039/c9en00710e.

Miura, N., Shinohara, Y., 2009. Cytotoxic effect and apoptosis induction by silver nanoparticles in HeLa cells. Biochem. Biophys. Res. Commun. 390, 733–737. https://doi.org/10.1016/j.bbrc.2009.10.039.

Petersen, S.J., 2017. Silver Nanoparticle Fate and Accumulation in the Aquatic Food Web of Stream Microcosms. ⟨https://digitalcommons.georgiasouthern.edu/etd/1656/⟩.

Piccinno, F., Gottschalk, F., Seeger, S., Nowack, B., 2012. Industrial production quantities and uses of ten engineered nanomaterials in Europe and the world. J. Nanopart. Res. 14, 1109. https://doi.org/10.1007/s11051-012-1109-9.

Polet, M., Laloux, L., Cambier, S., Ziebel, J., Gutleb, A.C., Schneider, Y.J., 2020. Soluble silver ions from silver nanoparticles induce a polarised secretion of interleukin-8 in differentiated Caco-2 cells. Toxicol. Lett. 325, 14–24. https://doi.org/10.1016/j.toxlet.2020.02.004.

Rubino, F., 2015. Toxicity of glutathione-binding metals: a review of targets and mechanisms. Toxics 3, 20–62. https://doi.org/10.3390/toxics3010020.

Schirmer, K., Chan, A.G.J., Greenberg, B.M., Dixon, D.G., Bols, N.C., 1997. Methodology for demonstrating and measuring the photocytotoxicity of fluoranthene to fish cells in culture. Toxicol. Vitr. 11, 107–119. https://doi.org/10.1016/S0887-2333(97)00002-7.

Schultz, A.G., Ong, K.J., MacCormack, T., Ma, G., Veinot, J.G.C., Goss, G.G., 2012. Silver nanoparticles inhibit sodium uptake in juvenile rainbow trout (Oncorhynchus mykiss). Environ. Sci. Technol. 46, 10295–10301. https://doi.org/10.1021/es3017717.

Simmons, S.O., Fan, C.Y., Yeoman, K., Wakefield, J., Ramabhadran, R., 2011. Nrf2 oxidative stress induced by heavy metals is cell type dependent. Curr. Chem. Genom. 5, 1–12. https://doi.org/10.2174/1875397301105010001.

Srivastava, M., Singh, S., Self, W.T., 2012. Exposure to silver nanoparticles inhibits selenoprotein synthesis and the activity of thioredoxin reductase. Environ. Health Perspect. 120, 56–61. https://doi.org/10.1289/ehp.1103928.

Sun, X., Yang, Y., Shi, J., Wang, C., Yu, Z., Zhang, H., 2017. NOX4- and Nrf2-mediated oxidative stress induced by silver nanoparticles in vascular endothelial cells. J. Appl. Toxicol. 37, 1428–1437. https://doi.org/10.1002/jat.3511.

Swain, P., Nayak, S.K., Sasmal, A., Behera, T., Barik, S.K., Swain, S.K., Mishra, S.S., Sen, A.K., Das, J.K., Jayasankar, P., 2014. Antimicrobial activity of metal based nanoparticles against microbes associated with diseases in aquaculture. World J. Microbiol. Biotechnol. 2491–2502. https://doi.org/10.1007/s11274-014-1674-4.

Tardillo Suárez, V., Karepina, E., Chevallet, M., Gallet, B., Cottet-Rousselle, C., Charbonnier, P., Moriscot, C., Michaud-Soret, I., Bal, W., Fuchs, A., Tucoulou, R., Jouneau, P.H., Veronesi, G., Deniaud, A., 2020. Nuclear translocation of silver ions and hepatocyte nuclear receptor impairment upon exposure to silver nanoparticles. Environ. Sci. Nano 7, 1374–1387. https://doi.org/10.1039/c9en01348b.

Thummabancha, K., Onparn, N., Srisapoome, P., 2016. Molecular characterization and expression analyses of cDNAs encoding the thioredoxin-interacting protein and selenoprotein P genes and histological changes in Nile tilapia (Oreochromis niloticus) in response to silver nanoparticle exposure. Gene 577, 161–173. https://doi.org/10.1016/j.gene.2015.11.031.

Tindell, R., Wall, S.B., Li, Q., Li, R., Dunigan, K., Wood, R., Tipple, T.E., 2018. Selenium supplementation of lung epithelial cells enhances nuclear factor E2-related factor 2 (Nrf2) activation following thioredoxin reductase inhibition. Redox Biol. 19, 331–338. https://doi.org/10.1016/j.redox.2018.07.020.

Tortella, G.R., Rubilar, O., Durán, N., Diez, M.C., Martínez, M., Parada, J., Seabra, A.B., 2020. Silver nanoparticles: toxicity in model organisms as an overview of its hazard for human health and the environment. J. Hazard. Mater. 390, 121974 https://doi.org/10.1016/j.jhazmat.2019.121974.

Turanov, A.A., Xu, X.-M., Carlson, B.A., Yoo, M.-H., Gladyshev, V.N., Hatfield, D.L., 2011. Biosynthesis of selenocysteine, the 21st amino acid in the genetic code, and a novel pathway for cysteine biosynthesis. Adv. Nutr. Int. Rev. J. 2, 122–128. https://doi.org/10.3945/an.110.000265.

Wood, C.M., 2011. Silver, Fish Physiology. Elsevier Inc. https://doi.org/10.1016/S1546-5098(11)31001-1

Xiao, B., Wang, X., Yang, J., Wang, K., Zhang, Y., Sun, B., Zhang, T., Zhu, L., 2020. Bioaccumulation kinetics and tissue distribution of silver nanoparticles in zebrafish: the mechanisms and influence of natural organic matter. Ecotoxicol. Environ. Saf. 194, 110454 https://doi.org/10.1016/j.ecoenv.2020.110454.

Yue, Y., Behra, R., Sigg, L., Fernández Freire, P., Pillai, S., Schirmer, K., 2015. Toxicity of silver nanoparticles to a fish gill cell line: role of medium composition. Nanotoxicology 9, 54–63. https://doi.org/10.3109/17435390.2014.889236.

Yue, Y., Li, X., Sigg, L., Suter, M.J.F., Pillai, S., Behra, R., Schirmer, K., 2017. Interaction of silver nanoparticles with algae and fish cells: a side by side comparison. J. Nanobiotechnol. 15, 1–11. https://doi.org/10.1186/s12951-017-0254-9.